ChemPlusChem

Research Article
doi.org/10.1002/cplu.202300020

Chemistry Europe
European Chemical Societies Publishing

www.chempluschem.org

Special Collection

# Mono- and Dinuclear Gold(I) Coumarin Complexes: Luminescence Studies and Singlet Oxygen Production

Carlota Sobrerroca,[a] Inmaculada Angurell,[a, b] Araceli de Aquino,[a, b] Guillermo Romo,[a, b] Camille Jubert,[a] and Laura Rodríguez*[a, b]

The 4-(thiolmethyl)-7-(diethylamino)-2H-chromen-2-one ligand has been synthesized and used as chromophore in several mono- and dinuclear gold(I) compounds that contain a phosphane at the second coordination position. Four final products were able to obtain in pure form containing one coumarin and one phosphane ligand in the case of PTA (1,3,5-triaza-7-phosphatricyclo[3.3.1.13.7]decane) and $PPh_3$ (triphenylphosphine); one coumarin and two gold(I)-phosphane groups in the case of phosphane = DAPTA (3,7-diacetyl-1,3,7-triaza-5-phosphabicyclo[3.3.1]nonane) and two coumarin and two gold(I) atoms in the case of phosphane = DPEphos (bis[(2-diphenylphosphino)phenyl]ether), when it was used a diphosphane. Other diphosphane ligands used were not able to give the desired products in pure form. The luminescent properties of the compounds are governed by the fluorescence of the coumarin moiety in all compounds both for measurements carried out in solution and also immobilized in PMMA organic matrix. Phosphorescence emission can be detected in all cases at 77 K both for the uncoordinated coumarin ligand and the gold(I) derivatives, being more favoured in the presence of the gold(I) heavy atom. The compounds have been used as photosensitizers to generate $^1O_2$ with moderate quantum yields values.

## Introduction

The development of luminescent materials is a research area of great interest in the last decades due to the large variety of applications on different fields such as electronic displays, luminescent switches, OLEDs, optical devices or sensing materials among others.[1–10] The presence of metal atoms, and particularly, transition metal atoms, in the chemical structure of the designed luminophores is increasing attention due to the intrinsic characteristics that can offer metals regarding enhanced optical properties and chemical configuration with larger variety of coordination numbers that can easily be tuned changing completely the resulting emission with respect to their energy (emission wavelength), intensity (quantum yields) and lifetimes. In particular, heavy atoms are especially relevant on luminescence since they are also very well-known to favor the intersystem crossing (ISC) process from $S_1$ to $T_1$ excited states. This may result on a change from fluorescence to phosphorescence emission (even at room temperature, producing room temperature phosphorescent materials) or generating energy transfer from $T_1$ to oxygen producing singlet oxygen, $^1O_2$.[11–13]

Gold(I) is one of the most relevant heavy atoms that is being studied on this field thanks to the possibility not only to favor ISC process but also to establish intermolecular gold(I)···gold(I) interactions. These interactions are responsible for the formation of large supramolecular assemblies and play a direct role also on the resulting luminescence.[13–19] Nevertheless, the presence of gold(I), as heavy atom, does not necessarily ensure a fast ISC rate, and the nature of the ligands also plays a key role in the excited-state and deactivation processes.[20–23] Hence, we can found gold(I) complexes that can act as pure phosphorescent emitters, as dual emitters (displaying fluorescence and phosphorescence in different ratios) or even also other cases where the observed emission is mainly due to the organic chromophore, resulting on pure fluorescence at room temperature.[24,25] Coumarins are very well-known chromophores that are included in this last group. In fact, coumarin derivatives have long been recognized on several biological applications,[26–30] especially antioxidant and anti-inflammatory activities and can be found in many drugs, and act as photocages to regulate biological processes.[31,32] Additionally, they have been used as dopants (blue, green and red) in organic light-emitting diodes (OLEDs) and also as probes or standards due to their high photostability and their wide range of fluorescence emission properties.[33]

Taking the interest of both gold(I) systems and coumarins, we have previously studied in our group some luminescent gold(I) coumarin complexes whose luminescence is mainly

[a] C. Sobrerroca, Dr. I. Angurell, A. de Aquino, G. Romo, C. Jubert, Prof. L. Rodríguez
Departament de Química Inorgànica i Orgànica
Secció de Química Inorgànica
Universitat de Barcelona
Martí i Franquès 1–11
08028 Barcelona (Spain)
E-mail: laura.rodriguez@qi.ub.es
[b] Dr. I. Angurell, A. de Aquino, G. Romo, Prof. L. Rodríguez
Institut de Nanociència i Nanotecnologia (IN2UB)
Universitat de Barcelona
08028 Barcelona (Spain)

Supporting information for this article is available on the WWW under https://doi.org/10.1002/cplu.202300020

Part of a Special Collection: "Ibero-American Women in Chemistry"

governed by the coumarin moiety. The photophysical properties of this type of compounds deserve more investigation due to the limited number of examples reported in the literature where the photophysics has been carefully analysed.[13,14,27,28,34,35] For this reason, in this work, we have designed and synthesized a new coumarin ligand containing a thiol terminal group suitable to be coordinated to a gold(I) atom. The use of thiol as linker will be also explored in order to compare the resulting emission and aggregation behaviour with respect to the previous compounds containing a propargyloxy group as connector. We expect that the angular geometry around the Au–S bond[36–38] with respect to the previous Au–C≡C should play a direct role on these parameters.

The second coordination position of the metal atom will be occupied by a phosphane (mono- or diphosphane) to modulate the resulting global properties of the final products both regarding stability, and luminescence. Based on previous work, we do not expect the formation of room temperature phosphorescent emitters, but the presence of the heavy atom may favour the population of the $T_1$ state and thus, the use of our molecules as photosensitizers to produce singlet oxygen has been also evaluated.

## Results and Discussion

### Synthesis and characterization

Coumarin ligand **L** has been synthesized according to the procedure shown in Scheme 1. Briefly, the oxidation of the commercial 7-diethylamino-4-methylcoumarin with selenium dioxide and subsequent reduction with sodium borohydride afforded the alcohol precursor **A**. It is worth mentioning that an exhaustive purification of the aldehyde derivative using column chromatography is needed before performing the reduction step. Precursor **A** was made react with mesyl chloride and LiBr to obtain the bromo-coumarin compound **B**. Finally, the reaction with thiourea yields the desired thiol-coumarin **L** in 40% global yield which was successfully characterized by IR, $^1$H and $^{13}$C{$^1$H} NMR spectroscopies and mass spectrometry.

The C=O stretching of the carbonyl at 1701 cm$^{-1}$, and S–H stretching at 2566 cm$^{-1}$ as a weak band, were clearly identified in the IR spectrum. $^1$H NMR spectrum displays the fingerprint of the thiol functionalization by the signals of the methylene attached to the thiol group as a doublet at 3.73 ppm, and those of the thiol group as a triplet at 1.87 ppm with a coupling constant around 8 Hz, apart from the protons of the coumarin rings and $NEt_2$ moiety. ESI mass spectrometry also confirmed the successful synthesis of the ligand, with the detection of $[M+H]^+$, $[M+Na]^+$ and $[M-H]^-$.

The ligand **L** was made react with different gold(I) sources ($AuCl(PR_3)$), being $PR_3 = PPh_3$, PTA, DAPTA, trimethylphosphane $PMe_3$ and triethylphosphane $PEt_3$) in order to obtain a series of phosphane-gold(I)-coumarin compounds that different on the solubility and steric hindrance of the $PR_3$ group. The reaction requires the deprotonation of the S–H group with potassium hydroxide as a base, in methanol, and the subsequent addition of a DCM solution of the $[AuCl(PR_3)]$ precursor (see Scheme 2). $PPh_3$ and PTA derivatives ([Au**L**(PTA)] **1a**, [Au**L**($PPh_3$)] **1b**) could be isolated in pure form while in the case of using the DAPTA phosphane, the 2:1 complex [{Au(DAPTA)}$_2$($\mu$-**L**)]Cl (**1c**) was obtained instead as identified by the $^1$H NMR and ESI-MS data (Figure 1). This compound presents the thiolate-coumarin ligand binding two gold atoms (see Scheme 2). Similar complexes with thiol ligands can be found in the literature.[39,40] Unfortunately, the reaction with $[AuCl(PMe_3)]$ and $[AuCl(PEt_3)]$ did not afford the desired compounds in pure form.

**1a** and **1b** were characterized by IR, $^1$H, $^{13}$C{$^1$H} and $^{31}$P{$^1$H} NMR spectroscopy and mass spectrometry. $^1$H NMR spectra show the signals of both, the coumarin ligand and the

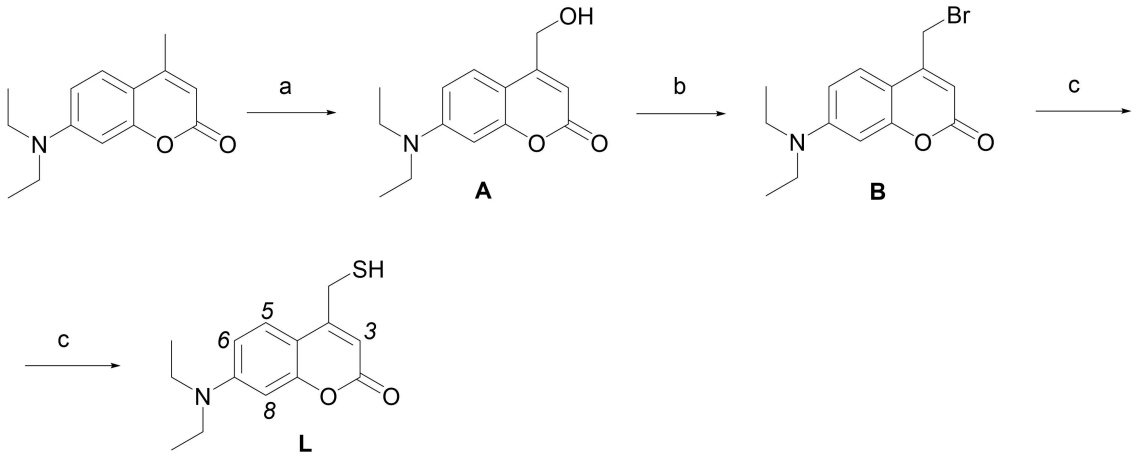


Reagents and conditions: (a) i) $SeO_2$, dioxane/$H_2O$, reflux, 14 days; ii)$NaBH_4$, ethanol, overhight; (b) i) MsCl, $NEt_3$, DCM, 2h; ii) LiBr, thf, 2h; (c) i) thiourea, ethanol/$Et_2O$, 2h at RT, 4h at 90ºC; ii) $NaOH_{(aq)}$.

**Scheme 1.** Schematic procedure for the synthesis of **L**.

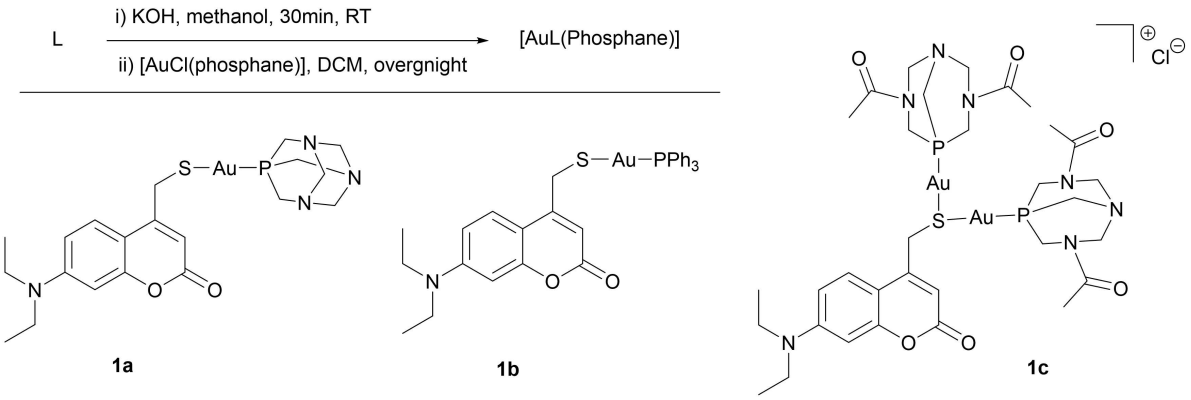


**Scheme 2.** Schematic procedure of the synthesis of **1 a**, **1 b** and **1 c**.

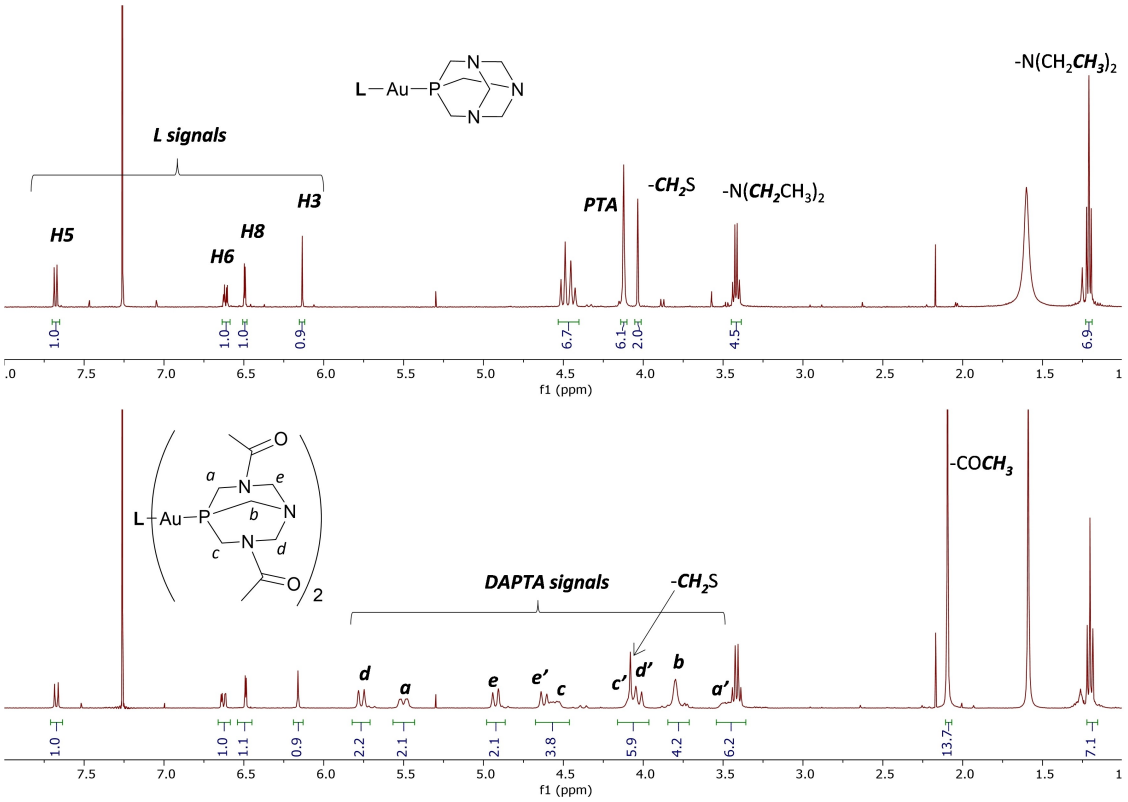


**Figure 1.** $^{1}$H NMR spectra of **1 a** (top) and **1 c** (bottom) in $CDCl_3$ displaying the different integration between the coumarin and the phosphane as a direct indication of different resulting compounds.

phosphane moiety with the expected 1:1 integration. The signal of the $CH_2S$ group downfield *ca.* 0.3 ppm due to the coordination to the gold atom, and the multiplicity of the signal changed from a triplet to a singlet due to the deprotonation of the thiol group. H*5* signal of the coumarin also downfield shifted significantly in both cases (see experimental section). $^{31}$P{$^{1}$H} NMR spectra show the presence of only one signal, at 38.3 ppm and −49.3 ppm for $PPh_3$ and PTA complexes, respectively, in agreement with similar published results.[41–44] The $^{13}$C{$^{1}$H} spectra show the resonances of both moieties. The signal of -$CH_2S$ appears downfield shifted after complex formation. The assignment of the resonances was made with $^{1}$H-$^{13}$C HSQC experiments (see Supporting Information). The mass spectra (HR ESI(+)) show for both compounds the molecular peak $[M+H]^+$.

On the other hand, the unexpected cationic **1 c** complex was identified by $^{1}$H NMR by the integration of the coumarin and the DAPTA moieties in the aforementioned 1:2 ratio (Figure 1). The proton H*5* of the coumarin, as well as the methylene $CH_2S$ group are downfield shifted upon the coordination to the gold(I) atom. The DAPTA signals appear in the 5.8–3.4 ppm range displaying the typical pattern of these protons. The assignment of the signals was made using HSQC experiments (see Figure S16). Again, in the $^{13}$C{$^{1}$H} NMR

spectrum (Figure S15) the signal of *C5* and $CH_2S$ appeared downfield shifted respect to the free ligand **L**. HR ESI(+) mass spectrometry showed in this case great fragmentation of the compound, and fragments corresponding at $[M\text{-}\{Au(DAPTA)\}+H]^+$ and $[M\text{-}\{Au(DAPTA)\}+Na]^+$ could be observed.

Concerning diphosphane derivatives, several chloridediphosphanegold(I) complexes with diphosphanes DPEphos (bis[(2-diphenylphosphino)phenyl]ether), xantphos (4,5-bis(diphenylphosphino)-9,9-dimethylxanthene), dppe (1,2-bisdiphenylphosphinoethane), dppm (bisdiphenylphosphinomethane), *trans*-dppen (trans-1,2-bis(diphenylphosphino)ethene), dppa (bis(diphenylphosphanyl)acetylene) were tested for the reaction with the thiol-coumarin ligand **L**, using the same experimental procedure as for monophosphane complexes but in a 1:2 (diphosphane: coumarin) stoichiometry (see Scheme 3). However, only in the case of the, DPEphos, a pure compound was obtained (**2**). $^{31}P\{^1H\}$ NMR spectrum showed the presence of only one signal at 28.8 ppm, 7 ppm downshifted with respect the gold(I) chloride precursor. $^1H$ NMR confirmed the obtaining of the desired complex and again, the coumarin signals shifted significatively respect the free ligand (Figure S20). HS ESI mass spectrometry show $[M+Na]^+$ signal at 1479.2603 confirming the proposed structure.

In the case of the complex containing the xantphos diphosphane, a mixture of compounds was obtained. In order to know how the reaction proceeded, the evolution of the mixture was followed by $^{31}P\{^1H\}$ NMR with an *inset* reference (see Figure 2). Starting from a solution of $[Au_2Cl_2(xantphos)]$, a solution in methanol of L + KOH (0.5 eq) was added; in 30 min a signal at 4.2 ppm corresponding to the bis(xantphos)gold(I) arises (**C**), as well as other signals at around 27 ppm that could be assigned to a compound with the thiol bridging two gold atoms **D**. The addition of another equivalent of thiolate ligand solution triggered the appearance of a new signal at 28.0 ppm corresponding to the initial expected $[Au_2L_2(xantphos)]$ compound (**E**), together with the bis(xantphos)gold(I) complex **C**. When the reaction was left reacting overnight new signals of decomposition appeared. Mass spectrometry confirmed the presence of **C** and **D** species.

Trying to avoid the formation of bis(xantphos)gold(I) species, the reaction was repeated but in more diluted conditions, and using the stoichiometric amount of **L**. Under these conditions, compound **E** could be obtained as the major product. However, $^{31}P\{^1H\}$ NMR showed the signal of **E** at 28 ppm as a broad signal, indicative of dynamic processes in solution.

Some modifications on the experimental procedures were explored in order to favor the formation of the unsuccessful diphosphane derivatives, such as increasing reaction time, changing solvent or adding excess of thiolate ligand but impure compounds were obtained in all cases. We cannot find any reason about the unexpected unsuccessful reaction for these dinuclear compounds.

## Photophysical characterization

Absorption and emission spectra of all compounds were recorded in $1\times10^{-5}$ M acetonitrile solutions and the results are summarized in Table 1 and Figure 3.

The absorption spectra of all compounds present a broad band at *ca.* 380 nm. This band corresponds to a $\pi$–$\pi^*$ absorption transition of the coumarin chromophore.[13,14,27,28,34,35,45–48] A second red-shifted transition

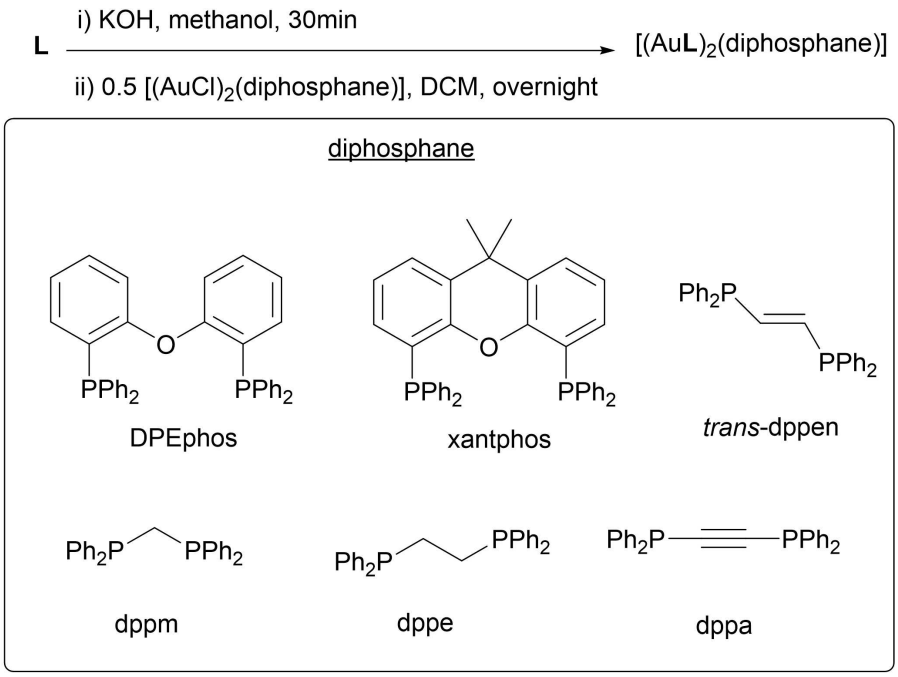


**Scheme 3.** Schematic procedure of the synthesis of $[Au_2L_2(diphosphane)]$ complexes.

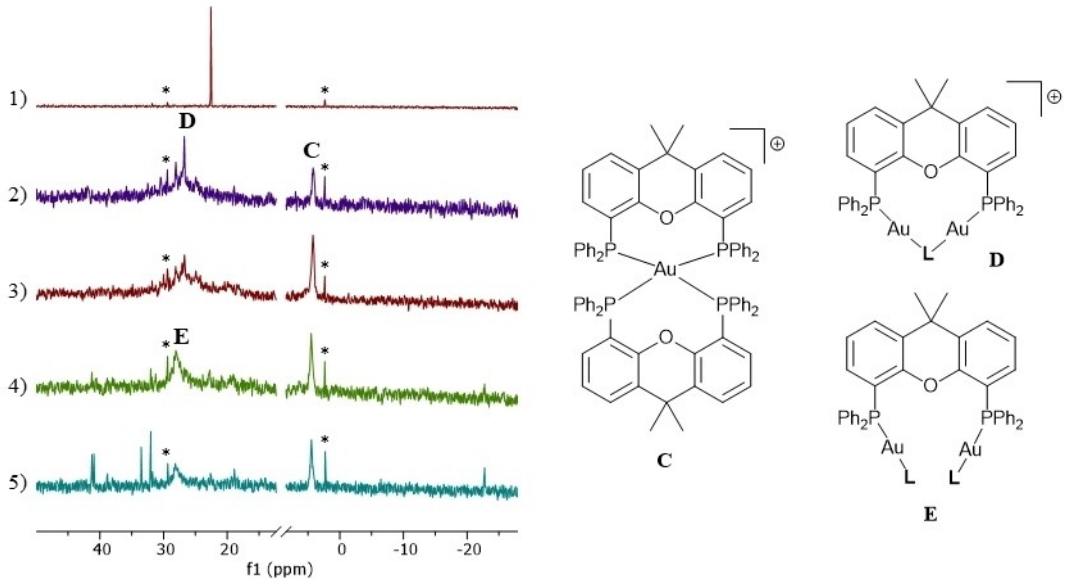


**Figure 2.** *Left:* Evolution of $^{31}P\{^{1}H\}$ NMR spectra of $[(AuCl)_2Xanthos]$ upon the addition of **L**. (1) $[(AuCl)_2Xanthos]$; (2) +0.5 equiv. of $L^-$, 30 min of reaction; (3) after 2 h of reaction; (4) +0.5 eq of $L^-$; (5) the same solution overnight. *Right:* proposed structures for **C**, **D** and **E**. *(* inset observed impurities)*

**Table 1.** Absorption and emission data of **L** and compounds **1a–c** and **2** gold(I) complexes in acetonitrile at $1\times10^{-5}$ M.

| Compound | Absorption $\lambda_{max}$ [nm] ($10^4$ ε [$M^{-1}cm^{-1}$]) | Fluorescence Emission, $\lambda_{exc}=380$ nm (solution, $\lambda_{max}$ [nm]) at RT |
|---|---|---|
| **L** | 382 (1.2) | 457 |
| **1a** | 378 (1.1) | 450 |
| **1b** | 378 (0.9) | 450 |
| **1c** | 381 (1.3) | 450 |
| **2** | 378 (2.8) | 450 |

with lower intensity is observed for the gold(I) compounds **1c** and **2** that could be ascribed to different conformers/dimers on the ground state where aurophilic interactions are involved[16] or to or a charge transfer transition in which a gold atom is involved.[5,49,50] The emission spectra of the compounds show the typical fluorescence band from the π–π* of the coumarin that is centred at *ca.* 450 nm, being 7 nm blue-shifted for the gold(I) complexes with respect to the emission of **L**[13,14,27,28,34,35,45]

The emission quantum yields are in all cases between 20–25% where there is not any relevant effect of the phosphane on the resulting emission efficiency but it is the double for gold(I) complexes in comparison with **L**, as previously observed in other gold(I)-coumarin derivatives.[13] Similar behaviour is observed in the emission lifetimes that are in all cases around 3.5 ns, in agreement with coumarin fluorescence that is not affected by the different phosphane environment (see below Table 2) being larger for gold(I) compounds with respect to **L**. Low temperature emission spectra display the presence of a

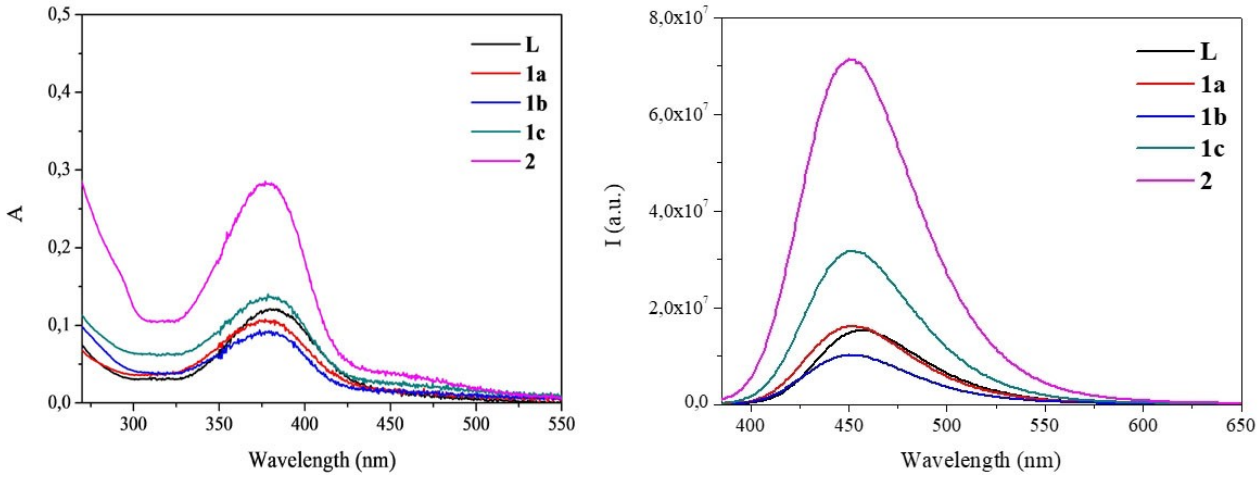


**Figure 3.** Absorption (left) and emission (right) spectra of **L**, **1a–c** and **2** in acetonitrile solutions at $1\times10^{-5}$ M.

**Table 2.** Fluorescence quantum yield ($\phi_{Fl}$) and lifetimes ($\tau$) values of **L** and **1 a–c** and **2** gold(I) complexes in acetonitrile:water mixtures at room temperature.[a] *The lifetime values of **L** are lower than the detection limit of our equipment.*

| % water | Compound | $\phi_{Fl}$ | $\tau$ [ns] | Compound | $\phi_{Fl}$ | $\tau$ [ns] |
|---|---|---|---|---|---|---|
| 0 | **L** | 0.10 | $<2$ ps[a] | **1 c** | 0.21 | 3.56 |
| 25 | | 0.07 | [a] | | 0.14 | 1.33 |
| 50 | | 0.05 | [a] | | 0.10 | 1.09 |
| 75 | | 0.04 | [a] | | 0.05 | 0.86 |
| 90 | | 0.04 | [a] | | 0.02 | 1.01 |
| 0 | **1 a** | 0.22 | 3.58 | **2** | 0.24 | 3.59 |
| 25 | | 0.13 | 1.41 | | 0.15 | 1.44 |
| 50 | | 0.09 | 1.31 | | 0.12 | 1.26 |
| 75 | | 0.05 | 1.41 | | 0.07 | 1.04 |
| 90 | | 0.02 | 1.54 | | 0.06 | 1.42 |
| 0 | **1 b** | 0.22 | 3.58 | | | |
| 25 | | 0.13 | 1.25 | | | |
| 50 | | 0.09 | 0.93 | | | |
| 75 | | 0.06 | 0.90 | | | |
| 90 | | 0.04 | 0.70 | | | |

phosphorescence $^3(\pi–\pi^*)$ band from the coumarin at 520–560 nm (Figure 4). This band is present in all compounds, being almost the solely emission for the gold(I) complexes while dual emission is recorded for **L**. This behaviour can be understood due to the heavy atom effect that enhances the triplet state population in the gold(I) compounds. Phosphorescence emission is not observed in deoxygenated samples at room temperature, as previously observed for other gold(I) coumarin compounds (Figure S24).[13]

Absorption and emission spectra were also recorded in all cases in acetonitrile/water mixtures in order to favour aggregation and analyse the resulting effects on their photophysics behaviour. All measurements were performed at 0, 25, 50, 75 and 90% water fraction ($f_w$) at the same concentration ($1\cdot10^{-5}$ M). In all cases, the absorption band is slightly red-shifted and decreasing on intensity for higher $f_w$ values together with an increase on the baseline. All these data agrees with the formation of small aggregates.[51]

The emission of the compounds is also red-shifted *ca.* 50 nm in all cases and results on a ca. 5-fold quenching in the case of **L** and 90% quenching for the gold(I) compounds (Figure 5 and S25–S29) in agreement with an Aggregation Caused Quenching (ACQ) behaviour. This is more relevant in the presence of gold(I) atoms as expected for the presence of this metal atoms that may favour aggregation due to the presence of additional weak possible contacts interactions (M···M interactions). The difference on ACQ is also evidenced in the quantum yields that, in the case of **L** is only reduced to the half while a 5–10% is reduced in the case of **1 a–c** and **2** (see Table 2). This behaviour is completely different from the one previously observed for other gold(I) coumarin derivatives that gives Aggregation Induced Emission (AIE) in similar mixture of solvents when using more flexible linker in the diphosphane and being the coumarin substituted at different position.[14] In fact, it is well known that the substitution of the coumarin plays a key role on the resulting photophysical properties and we can observe herein that it also plays an important role with regard to the resulting ACQ or AIE behaviour.

The resulting quenching can be ascribed to an increase on the non-radiative pathways ($k_{nr}$) as observed on the decrease of both the quantum yields and lifetimes when the amount of water on the samples increases (see Table S1). The emission lifetimes of the aggregates are also lower than the corresponding monomers and decrease when the aggregation is more favoured (larger amount of water, see Table 2). This is clearly reflected in a global increase (3 to 5-fold) of the $k_{nr}$ in the aggregated samples (Table S1).

Nevertheless, not only the coumarin group must play a key role in this aggregation process (ACQ vs the previous AIE). The linking unit is also different in this case compared to the previous work of the group where the chromophore (coumarin) was coordinated to the gold(I) atom through a propargyloxy

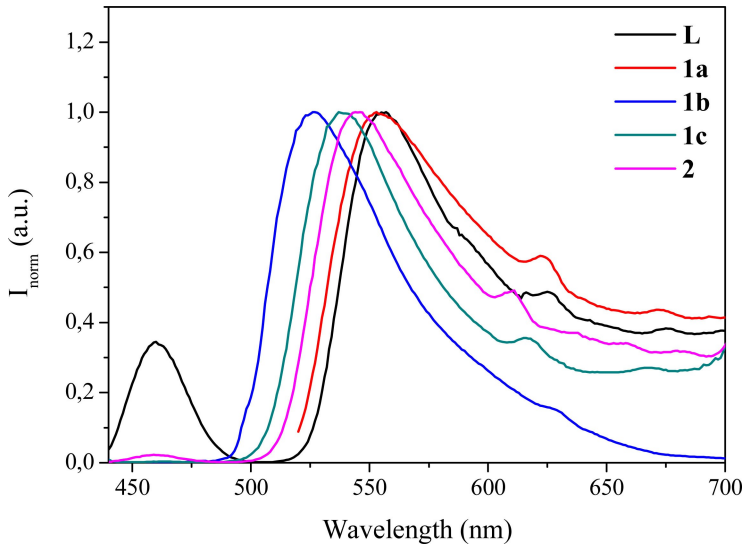


**Figure 4.** Normalized emission (right) spectra of **L**, **1 a–c** and **2** in acetonitrile solutions at $1\times10^{-5}$ M and 77 K.

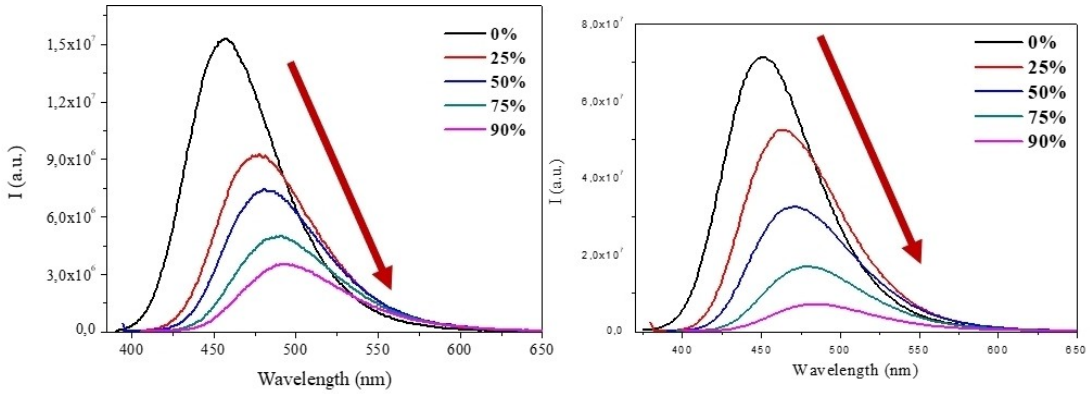


**Figure 5.** Emission spectra of **L** (left) and **1 a** (right) at $1 \cdot 10^{-5}$ M concentration using different water contents (mixture with acetonitrile). The water percentage is indicated in the legend.

moiety. That is, the geometry around the metal atom is different being linear (due to the direct Au-alkynyl coordination) in the previous work and angular in the current studies. Hence, the final disposition of the chromophore has been demonstrated to play a key role on the resulting effect on the emission of the aggregates.

### Singlet Oxygen production

The detection of the coumarin phosphorescence emission encouraged us to test our compounds as singlet oxygen photosensitizers. The experiments were carried out by the detection of the phosphorescence emission of the $^1O_2$ at *ca.* 1270 nm using perinaphthenone as standard reference ($\phi_\Delta = 0.79$). The highest value has been recorded for the dinuclear compound containing the DAPTA phosphane (**1 c**) where the two gold(I) metal atoms are coordinated to the same sulphur unit (Table 3). This can be due to the stronger intersystem crossing effect produced to the same coumarin chromophore in comparison with the other compounds where one atom is close coordinated to one chromophore. These values agree with previous data of singlet oxygen production with gold(I) complexes containing coumarin as chromophore.[13,14] Previous $\phi_\Delta$ values obtained with gold(I) coumarin compounds were in the order of ca. 2–15 %. Thus, the use of thiol linkers instead of propargyloxy moiety (and corresponding different geometry of the complexes) and the $NEt_2$ group do not seem to affect substantially the production of singlet oxygen.

### Luminescent materials

The compounds were dispersed in PMMA in order to prepare luminescent materials using 1 % and 5 % relative mass of the luminophores within the organic matrix. As observed in Figures 6 and S30 and Table 4, the emission efficiency is higher using 1 % of doping agents. As a general trend, the nuclearity seems to negatively affect the resulting emission intensity while it is not affecting the luminescent decay times. This has been ascribed to a decrease on the radiative fluorescence channel ($k_r$) in the presence of the heavy atoms (Table S3) in agreement with the enhanced population of the $T_1$ state responsible for phosphorescence, as previously demonstrated (Figure 4).

Emission lifetimes and quantum yields are similar to those recorded in pure acetonitrile solution but the lifetimes are slightly larger than those recorded in the aggregated acetonitrile/water samples. We can suggest that the molecules are well-dispersed in PMMA minimized the formation of non-emissive aggregates.

Comparison of the photophysical properties in solution and in PMMA let us to observe that, contrary to what is commonly observed, the photophysical properties of the compounds are not substantially affected when they are dispersed in PMMA. That is, we have managed to maintain the same or very similar emissive characteristics (emission wavelength, quantum yields and decay times) but going from solution to the solid state.

**Table 3.** Singlet oxygen production quantum yields ($\phi_\Delta$) calculated for all the compounds.

| Compound | $\phi_\Delta$ [%] |
|---|---|
| **L** | 1.1 |
| **1 a** | 2.0 |
| **1 b** | 1.3 |
| **1 c** | 10.3 |
| **2** | 3.7 |

**Table 4.** Quantum yields (QY) and lifetime (τ) values for **L** and gold complexes in PMMA using 1 % of doping agent.

| Compound | $\lambda_{em}$ | $\phi$ 1 % PMMA | τ 1 % PMMA [ns] |
|---|---|---|---|
| **L** | 440 | 0.08 | 2.25 |
| **1 a** | 433 | 0.05 | 2.67 |
| **1 b** | 442 | 0.04 | 2.67 |
| **1 c** | 439 | 0.03 | 2.34 |
| **2** | 439 | 0.02 | 2.46 |

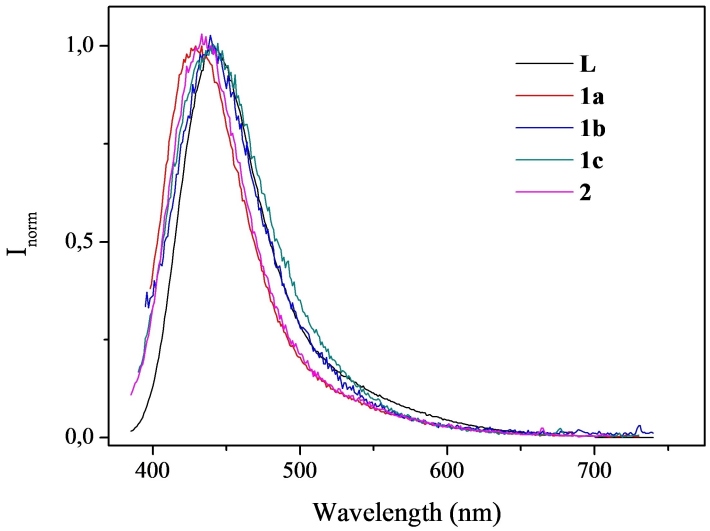


**Figure 6.** Emission of the PMMA matrixes doped with the compounds at 1% mass amount of chromophore.

## Conclusions

The use of different monophosphanes can direct the formation of either mono- or dinuclear gold(I) complexes containing a coumarin chromophore with a thiol group as coordinating position. We have obtained one or two gold-phosphane moieties coordinated to a sulphur atom. The formation of pure dinuclear compounds resulted more difficult in some cases with respect to mononuclear compounds precluding their photophysical study.

All compounds are luminescent being the emission governed directly by the coumarin intraligand transitions that give place to fluorescent emission (at room temperature). Phosphorescent emission has been recorded for both the free coumarin ligand and the gold(I) complexes at 77 K, being more favoured in the presence of the gold(I) heavy atom.

The compounds aggregate in acetonitrile:water mixtures giving rise to quenched assemblies.

They have been also tested as singlet oxygen photosensitizers in acetonitrile giving rise to moderate values where the presence of two gold(I) atoms directly coordinated to one chromophoric unit (compound **1c**) is affecting clearly the quantum yield of this process being 5-fold higher than for the rest of the compounds.

The immobilization of the samples in PMMA matrix let us to obtain luminescent materials where the emission decay times are not affected by the presence of the heavy atom.

## Experimental Section

### General Procedures

All manipulations have been performed under prepurified $N_2$ using standard Schlenk-tube techniques. All solvents have been distilled from appropriate drying agents. Alternatively, a solvent purification system (Innovative Technologies) was also used. Literature methods were used to prepare **A**[52] and **B**.[53] The phosphane gold chlorido precursors [AuCl(PTA)], [AuCl($PPh_3$)], [AuCl(DAPTA)], [$(AuCl)_2$(DPEphos)], [$(AuCl)_2$(xantphos)], [$(AuCl)_2$(dppm)], [$(AuCl)_2$(dppe)], [$(AuCl)_2$(*trans*-dppen)], and [$(AuCl)_2$(dppa)] were prepared from the reaction of [AuCl(tht)] with the appropriate phosphane. All other reagents were obtained from commercial suppliers and used as received.

Infrared spectra have been recorded on an FTIR Nicolet™ iS™ 5 Spectrophotometer. $^1$H NMR (δ(TMS) = 0.0 ppm) and $^{31}$P{$^1$H} NMR (δ(85% $H_3PO_4$) = 0.0 ppm) spectra were recorded at 400 or 500 MHz using Varian and Bruker spectrometers at 25 °C. ESI mass spectra were recorded on a Fisons VG Quatro spectrometer. Absorption spectra have been recorded on a Varian Cary 100 Bio UV Spectrophotometer, and emission spectra on a Horiba-Jobin-Ybon SPEX Nanolog Spectrofluorimeter. Quantum yields have been recorded on a Hamamatsu Absolute PL Quantum Yield Spectrometer C11347. Luminescence lifetimes were measured on a JYF-DELTAPRO-NL equipment upon excitation of the samples with a 280 nm NanoLED and collecting the decays through a bandpass filter of 400 nm.

### Synthesis and characterization

***Synthesis of L.*** To a solution of 4-(bromomethyl)-7-(diethylamino)-2H-chromen-2-one (0.431 g, 1.39 mmol) in 80 mL of a mixture of ethanol: ether (1:1) thiourea (0.106 g, 1.39 mmol) was added, and the mixture was stirred at room temperature for 2 h, and then, it was heated to 90 °C for 4 h. Next, half of the volume was evaporated, and 30 mL of 5% aqueous solution of NaOH was added. After, the solution was neutralized with HCl 1 M, the product was extracted with $CH_2Cl_2$ (3 × 50 mL) and the organic layer was washed with water (20 mL), dried with $MgSO_4$ anhydrous, and evaporated to dryness. An orange oily solid was obtained. 68% yield (0.249 g).

IR ($cm^{-1}$): 3072 ν($C_{sp2}$–H); 2968, 2927 ν($C_{sp3}$–H); 2566 ν(S–H); 1701 ν(C=O); 1590, 1523 (C=$C_{ar}$).

$^1$H NMR (500 MHz, $CDCl_3$): δ (ppm) = 7.43 (d, J = 9 Hz, 1H, $^5$CH), 6.61 (dd, J = 9 Hz, J = 2.5 Hz, 1H, $^6$CH), 6.52 (d, J = 2.5 Hz, 1H, $^8$CH), 6.09 (s, 1H, $^3$CH), 3.73 (d, J = 8 Hz, 2H, $CH_2$S), 3.42 (q, J = 7 Hz, 4H, N($CH_2CH_3$)$_2$), 1.87 (t, J = 8 Hz, 1H, SH), 1.21 (t, J = 7 Hz, 6H, N-($CH_2CH_3$)$_2$). $^{13}$C{$^1$H} NMR (500 MHz, $CDCl_3$): δ = 162.3 (C), 156.8 (C),

154.5 (C), 150,8 (C), 125.3 ($^5$C), 108.7 ($^6$C), 107.0 ($^3$C), 106.7 (C), 98.1 ($^8$C), 44.9 (N($CH_2CH_3$)$_2$), 25.1 ($CH_2$S), 12.6 (N($CH_2CH_3$)$_2$). ESI-MS(+) *m/z*: 549.18 [2 M + Na]$^+$ (calcd. 549.18); 527.20 [2 M + H]$^+$ (calc. 527.20); 286.09 [M + Na]$^+$ (calc. 286.09); 264.11 [M + H]$^+$ (calc. 264.11). ESI-MS(−): 262.09 [M−H]$^-$ (calc. 262.09).

***Synthesis of 1a.*** A solution of **L** (28 mg, 0.11 mmol) and KOH (12 mg, 0.21 mmol) in 10 mL of MeOH was stirred for 30 min at room temperature. Then, a solution of [AuCl(PTA)] (42 mg, 0.11 mmol) in 10 mL of dichloromethane was added and the resulting solution was stirred overnight. The solvent was evaporated almost to dryness and the product was precipitated with $Et_2O$. The solid obtained was filtered and recrystallized in dichloromethane/hexane. **1a** was obtained as a yellow solid in 51% yield.

IR (cm$^{-1}$): 2975, 2922 ν($C_{sp3}$–H); 1704 ν(C=O); 1596, 1523 (C=$C_{ar}$). $^1$H NMR (500 MHz, $CDCl_3$): δ (ppm) = 7.67 (d, *J* = 9.0 Hz, 1H, $^5$CH), 6.61 (dd, *J* = 9 Hz, *J* = 3 Hz, 1H, $^6$CH), 6.49 (d, J = 3 Hz, 1H, $^8$CH), 6.13 (s, 1H, $^3$CH), 4.47 (m, 6H, $CH_2$), 4.12 (s, 6H, $CH_2$), 4.03 (s, 2H, $CH_2$S), 3.42 (q, *J* = 7 Hz, 4H, N($CH_2CH_3$)$_2$), 1.20 (t, *J* = 7 Hz, 6H, N($CH_2CH_3$)$_2$). $^{31}$P{$^1$H} NMR (202 MHz, $CDCl_3$): δ −49.3 ppm. $^{13}$C{$^1$H} NMR (125 MHz, $CDCl_3$): δ = 163.2 (C), 162.0 (C), 157.0 (C), 150.7 (C), 126.8 ($^5$C), 108.6 (6 C), 107.6 (C), 107.4 ($^3$C), 97.9 ($^8$C), 73.4 (d, *J* = 9.5 Hz, $CH_2$), 52.7 (d, *J* = 23.8 Hz, $CH_2$), 44.9 (N($CH_2CH_3$)$_2$), 28.4 ($CH_2$S), 12.7 (N($CH_2CH_3$)$_2$). HR ESI-MS(+) *m/z*: 617.1420 [M + H]$^+$ (calc. 617.1414); 158.0841 [PTA + H]$^+$ (calc. 158.0847); 264.1055 [L + H]$^+$ (calc. 264.1058).

***Synthesis of 1b.*** The same procedure as **1a** was followed but using 40 mg (0.15 mmol) of **L**, 17 mg (0.30 mmol) of KOH, and 76 mg (0.15 mmol) of [AuCl($PPh_3$)]. 1b was obtained as a yellow solid in 30% yield.

IR (cm$^{-1}$): 3054 ($C_{sp2}$–H); 2964 ν($C_{sp3}$–H); 1705 ν(C=O); 1610, 1595 (C=$C_{ar}$). $^1$H NMR (400 MHz, $CDCl_3$): δ (ppm) = 7.81 (d, *J* = 8.8 Hz, 1H, $^5$CH), 7.52-7.36 (m, 15H, Ph), 6.47 (dd, *J* = 8.8 Hz, *J* = 2.4 Hz, 1H, $^6$CH), 6.42 (d, *J* = 2.4 Hz, 1H, $^8$CH), 6.18 (s, 1H, $^3$CH), 4.13 (s, 2H, $CH_2$S), 3.33 (q, *J* = 7.2 Hz, 4H, N($CH_2CH_3$)$_2$), 1.13 (t, *J* = 7.2 Hz, 6H, N($CH_2CH_3$)$_2$). $^{31}$P{$^1$H} NMR (162 MHz, $CDCl_3$): δ = 38.3 ppm. $^{13}$C{$^1$H} NMR (125 MHz, $CDCl_3$): δ = 163.1 (C), 161.4 (C), 156.9 (C), 150.5 (C), 134.3 (d, *J* = 13.6 Hz, *o*-Ph), 131.7 (d, *J* = 2 Hz, *p*-Ph), 129.8 (*ipso*-Ph), 129.3 (d, *J* = 11.4 Hz, *m*-Ph), 127.0 ($^5$C), 108.6 ($^6$C), 107.7 (C), 107.2 ($^3$C), 97.9 ($^8$C), 44.8 (N($CH_2CH_3$)$_2$), 28.8 ($CH_2$S), 12.7 (N($CH_2CH_3$)$_2$). HR ESI-MS(+) *m/z*: 722.1539 [M + H]$^+$ (calc. 722.1557); 744.1365 [M + Na]$^+$ (calc. 744.1376); 721.1466 [Au($PPh_3$)$_2$]$^+$ (calc. 722.1488); 1180.2048 [2 M−$PPh_3$]$^+$ (calc. 1180.2046).

***Synthesis of 1c.*** The synthesis of **1c** was performed following the same procedure as that for **1a** using 44 mg (0.17 mmol) of **L**, 19 mg (0.34 mmol) of KOH, and 77 mg (0.17 mmol) of [AuCl(DAPTA)]. **1c** was obtained as a yellow solid in 59% yield.

IR (cm$^{-1}$): 2962 ν($C_{sp3}$–H); 1698 ν(C=O); 1608, 1528 ν(C=O) and ν (C=$C_{ar}$). $^1$H NMR (400 MHz, $CDCl_3$): δ(ppm) = 7.67 (d, *J* = 9.0 Hz, 1H, $^5$CH), 6.63 (dd, *J* = 9.0 Hz, J = 2.6 Hz, 1H, $^6$CH), 6.49 (d, J = 2.6 Hz, 1H, $^8$CH), 6.16 (s, 1H, $^3$CH), 5.76 (d, J = 14.2 Hz, 2H, N-$^d$$CH_2$-N), 5.50 (d, J = 16 Hz, 2H, P-$^a$$CH_2$-N), 4.92 (d, J = 14.0 Hz, 2H, N-$^e$$CH_2$-N), 4.64-4.50 (m, 4H, P-$^c$$CH_2$-N + N-$^{e'}$$CH_2$-N), 4.10–3.98 (m, 6H, P-$^{c'}$$CH_2$-N, N-$^{d'}$$CH_2$-N, $CH_2$S), 3.80 (s, 4H, P-$^b$$CH_2$-N), 3.50 (m, 2H, P-$^{a'}$$CH_2$-N), 3.42 (q, J = 7.1 Hz, 4H, N($CH_2CH_3$)$_2$), 2.01 (s, 12H, CO$CH_3$), 1.20 (t, J = 7.1 Hz, 6H, N($CH_2CH_3$)$_2$). $^{31}$P{$^1$H} NMR (162 MHz, $CDCl_3$): δ = -38.9 ($s_{br}$). $^{13}$C{$^1$H} NMR ($CDCl_3$, 125): δ = 1702 (C=O), 169.8 (C=O), 138.3 (C), 126.7 ($^5$C), 108.8 ($^6$C), 107.3 ($^3$C), 97.8 ($^8$C), 67.5 (N-$^e$$CH_2$-N), 62.2 (N-$^d$$CH_2$-N), 49.2 (d, *J* = 20.8 Hz, P-$^b$$CH_2$-N), 44.9 (N($CH_2CH_3$)$_2$), 44.5 (P-$^c$$CH_2$-N), 39.4 (d, *J* = 21.5 Hz, P-$^a$$CH_2$-N), 28.8 ($CH_2$S), 21.7 (s, CO$CH_3$), 21.4 (s, CO$CH_3$'), 12.7 (N($CH_2CH_3$)$_2$). HR ESI-MS(+) *m/z*: 711.1453 [M−{Au-(DAPTA)} + Na]$^+$ (calc., 711.1445); 689.1608 [M-{Au(DAPTA)} + H]$^+$ (calc. 689.1626); 549.1849 [2 L + Na]$^+$, 527.2038 [2 L + H]$^+$, 481.1857 [2DAPTA + Na]$^+$, 459.2051 [2DAPTA + H]$^+$, 264.106 [L + H]$^+$, 252.0879 [DAPTA + Na]$^+$, 230.1057 [DAPTA + H]$^+$.

***Synthesis of 2.*** The same procedure described before for **1a** was followed but using 40 mg (0.15 mmol) of **L**, 17 mg (0.30 mmol) of KOH and 76 mg (0.076 mmol) of [$(AuCl)_2$(dpephos)]. Yield: 84%.

IR: 3053 ($C_{sp2}$–H); 2964 ν($C_{sp3}$–H); 1700 ν(C=O); 1609, 1592 (C=$C_{ar}$). $^1$H NMR (500 MHz, $CDCl_3$): δ (ppm) = 7.77 (d, *J* = 9.0 Hz, 2H, $^5$CH), 7.39 (m, 16H, CH), 7.18–7.04 (m, 12H, CH), 6.86 (dd, *J* = 8.0 Hz, *J* = 5 Hz, 2H, CH), 6.65 (ddd, *J* = 11 Hz, *J* = 7 Hz, *J* = 1.5 Hz, 2H, CH), 6.41 (d, *J* = 2.5 Hz, 2H, $^8$CH), 6.34 (dd, *J* = 9 Hz, *J* = 2.5 Hz, 2H, $^6$CH), 6.13 (s, 2H, $^3$CH), 4.01 (s, 4H, $CH_2$S), 3.28 (m, 8H, N($CH_2CH_3$)$_2$), 1.10 (t, *J* = 7 Hz, 12H, N($CH_2CH_3$)$_2$). $^{31}$P{$^1$H} NMR (202 MHz, $CDCl_3$): δ = 28.8. HR ESI-MS(+) *m/z*: 1479.2603 [M + Na]$^+$ (calc. 1479.2648); 1194.1828 [M−L]$^+$ (calc. 1194.1848).

### Preparation of acetonitrile:water mixtures

A 3 mL stock solution of all compounds in acetonitrile with an absorption of 0.5–0.6 (at 320 nm) in a 10 mm quartz cuvette was prepared. An aliquot (200 μL) of the stock solution was transferred to a 2 mL volumetric flask. After the appropriate amount of acetonitrile was added, water was added to furnish mixtures with different water fractions (fw = 0–90% by volume) with the same compound concentrations. The photophysical studies of the resultant mixtures were performed immediately after the sample preparation.

### Singlet oxygen quantum yields ($\phi_\Delta$) measurement

Room-temperature singlet oxygen phosphorescence was detected at 1270 nm with a Horiba-Jobin-Ybon SPEX Nanolog spectrofluorimeter (Universitat de Barcelona) using the DSS-IGA020L detector. The use of a Schott RG 1000 filter was essential to eliminate from the infrared signal all the first harmonic contribution of sensitizer emission in the region below 850 nm. The singlet oxygen formation quantum yield was then determined by direct measurement of the phosphorescence at 1270 nm following irradiation of the aerated aqueous dispersions of the samples. The samples were adjusted to an absorption nearly to 1 respect to excitation wavelength to increase the sensitivity of the detection. Perinaphthenone in dichloromethane was used as standard reference, applying equation (1).

$$\Delta = {}^{ref}_{\Delta} \frac{Emission_{1270\ nm}}{Emission^{ref}_{1270\ nm}} \quad (1)$$

with ${}^{ref}_{\Delta}$ the singlet oxygen formation quantum yield of the reference compound ( ${}^{ref}_{\Delta} = 0.79$). The integration area of the emissions recorded at 1270 nm were used for the calculations.

### Preparation with PMMA doped matrixes

The films were prepared via drop-casting, using a mixture of dopant and PMMA. Polymer solutions were prepared as follows: PMMA solution was prepared (MW 120000, 300 mg/mL solution in dichloromethane). To a 100 μL of polymer solution was added to the same volume a solution of the sample at a concentration of 20 μg/mL. The films were drop-cast onto a quartz substrate at room temperature to avoid any thermal annealing.

## Acknowledgements

*The authors are grateful to projects PID2019-104121GB–I00 funded by the Ministerio de Ciencia e Innovación of Spain MCIN/*

*AEI/10.13039/501100011033. G.R.-I. acknowledge Fundación Carolina and Secretaría de Relaciones Exteriores de México for the Ph.D. Scholarship.*

## *Conflict of Interest*

*There are no conflicts to declare.*

## Data Availability Statement

The data that support the findings of this study are available in the Supporting Information of this article.

**Keywords:** coumarin · gold(I) · luminescence · polymer matrices · singlet oxygen

[1] V. W. W. Yam, E. C. C. Cheng, *Chem. Soc. Rev.* **2008**, *37*, 1806–1813.
[2] J. C. Lima, L. Rodríguez, *Inorganics* **2019**, *7*, 1–12.
[3] M. Pujadas, L. Rodríguez, *Coord. Chem. Rev.* **2020**, *408*, 213179.
[4] A. Pinto, M. Echeverri, B. Gómez-Lor, L. Rodríguez, *Dyes Pigm.* **2022**, *202*, 1–12.
[5] A. de Aquino, F. J. Caparrós, G. Aullón, K. N. Truong, K. Rissanen, J. C. Lima, L. Rodríguez, *Dalton Trans.* **2022**, 16282–16291.
[6] I. Soldevilla, M. Santamaría-Paganini, M. E. Olmos, M. Monge, J. M. López-de-Luzuriaga, M. Rodríguez-Castillo, *Appl. Organomet. Chem.* **2022**, 1–9.
[7] I. Soldevilla, A. García-Camacho, R. T. Nasibullin, M. E. Olmos, M. Monge, D. Sundholm, R. R. Valiev, J. M. López-De-Luzuriaga, M. Rodríguez-Castillo, *J. Mater. Chem. C* **2022**, *10*, 4894–4904.
[8] D. Blasco, J. M. López-De-Luzuriaga, M. Monge, M. E. Olmos, M. Rodríguez-Castillo, H. Amaveda, M. Mora, V. García Sakai, J. A. Martínez-González, *Inorg. Chem. Front.* **2021**, *8*, 3707–3715.
[9] J. C. Lima, L. Rodríguez, *Chem. Soc. Rev.* **2011**, *40*, 5442–5456.
[10] M. Rosental, R. N. Coldman, A. J. Moro, I. Angurell, R. M. Gomila, A. Frontera, J. C. Lima, L. Rodríguez, *Molecules* **2021**, *26*, 1–14.
[11] A. De Aquino, J. S. Ward, K. Rissanen, G. Aullón, J. C. Lima, L. Rodríguez, *Inorg. Chem.* **2022**, *61*, 20931–20941.
[12] A. Pinto, J. S. Ward, K. Rissanen, M. Smith, L. Rodríguez, *Dalton Trans.* **2022**, *51*, 8795–8803.
[13] A. Pinto, C. Cunha, G. Aullón, J. C. Lima, L. Rodríguez, J. S. Seixas de Melo, *J. Phys. Chem. B* **2021**, *125*, 11751–11760.
[14] C. Cunha, A. Pinto, A. Galvão, L. Rodríguez, J. S. Seixas de Melo, *Inorg. Chem.* **2022**, *61*, 6964–6976.
[15] J. C. Lima, L. Rodríguez, *Inorganics* **2015**, *3*, 1–18.
[16] L. Rodríguez, M. Ferrer, R. Crehuet, J. Anglada, J. C. Lima, *Inorg. Chem.* **2012**, *51*, 7636–7641.
[17] S. Sculfort, P. Braunstein, *Chem. Soc. Rev.* **2011**, *40*, 2741–2760.
[18] H. Schmidbaur, A. Schier, *Chem. Soc. Rev.* **2012**, *41*, 370–412.
[19] M. Casciotti, G. Romo-Islas, M. Álvarez, F. Molina, J. M. Muñoz-Molina, T. R. Belderrain, L. Rodríguez, *Dalton Trans.* **2022**, *51*, 17162–17169.
[20] A. Belyaev, I. Kolesnikov, A. S. Melnikov, V. V. Gurzhiy, S. P. Tunik, I. O. Koshevoy, *New J. Chem.* **2019**, *43*, 13741–13750.
[21] A. Gutiérrez-Blanco, V. Fernández-Moreira, M. C. Gimeno, E. Peris, M. Poyatos, *Organometallics* **2018**, *37*, 1795–1800.
[22] Y. Y. Chia, M. G. Tay, *Dalton Trans.* **2014**, *43*, 13159–13168.
[23] E. Aguiló, A. J. Moro, M. Outis, J. Pina, D. Sarmento, J. S. Seixas de Melo, L. Rodríguez, J. C. Lima, *Inorg. Chem.* **2018**, *57*, 13423–13430.
[24] A. de Aquino, F. J. Caparrós, K. N. Truong, K. Rissanen, M. Ferrer, Y. Jung, H. Choi, J. C. Lima, L. Rodríguez, *Dalton Trans.* **2021**, *50*, 3806–3815.
[25] A. de Aquino, F. J. Caparrós, G. Aullón, J. S. Ward, K. Rissanen, Y. Jung, H. Choi, J. C. Lima, L. Rodríguez, *Chem. A Eur. J.* **2021**, *27*, 1810–1820.
[26] Y. F. Sun, S. H. Xu, R. T. Wu, Z. Y. Wang, Z. B. Zheng, J. K. Li, Y. P. Cui, *Dyes Pigm.* **2010**, *87*, 109–118.
[27] J. Arcau, V. Andermark, E. Aguiló, A. Gandioso, A. Moro, M. Cetina, J. C. Lima, K. Rissanen, I. Ott, L. Rodríguez, *Dalton Trans.* **2014**, *43*, 4426–4436.
[28] R. Gavara, E. Aguiló, J. Schur, J. Llorca, I. Ott, L. Rodríguez, *Inorg. Chim. Acta* **2016**, *446*, 189–197.
[29] M. J. Matos, D. Viña, E. Quezada, C. Picciau, G. Delogu, F. Orallo, L. Santana, E. Uriarte, *Bioorg. Med. Chem. Lett.* **2009**, *19*, 3268–3270.
[30] S. Lee, K. Sivakumar, W. S. Shin, F. Xie, Q. Wang, *Bioorg. Med. Chem. Lett.* **2006**, *16*, 4596–4599.
[31] R. Klimek, M. Asido, V. Hermanns, S. Junek, J. Wachtveitl, A. Heckel, *Chem. A Eur. J.* **2022**, *28*, e202200647.
[32] A. Pinheiro, P. Baptistap, J. C. Lima, *Nucleic Acids Res.* **2008**, *36*, e90.
[33] B. D. Wagner, *Molecules* **2009**, *14*, 210–237.
[34] A. J. Moro, B. Rome, E. Aguiló, J. Arcau, R. Puttreddy, K. Rissanen, J. C. Lima, L. Rodríguez, *Org. Biomol. Chem.* **2015**, *13*, 2026–2033.
[35] A. Pinto, J. Sonet, R. M. Gomila, A. Frontera, J. C. Lima, L. Rodríguez, *Inorg. Chem. Front.* **2022**, *9*, 6047–6060.
[36] A. Gutiérrez, I. Marzo, C. Cativiela, A. Laguna, M. C. Gimeno, *Chem. A Eur. J.* **2015**, *21*, 11088–11095.
[37] I. O. Koshevoy, E. S. Smirnova, M. Haukka, A. Laguna, J. Camara Chueca, T. A. Pakkanen, S. P. Tunik, I. Ospino, O. Crespo, *Dalton Trans.* **2011**, *40*, 7412–7422.
[38] H. Goitia, Y. Nieto, M. D. Villacampa, C. Kasper, A. Laguna, M. C. Gimeno, *Organometallics* **2013**, *32*, 6069–6078.
[39] J. Quero, S. Cabello, T. Fuertes, I. Mármol, R. Laplaza, V. Polo, M. C. Gimeno, M. J. Rodriguez-Yoldi, E. Cerrada, *Inorg. Chem.* **2018**, *57*, 10832–10845.
[40] B. Wu, X. Yang, M. Yan, *J. Med. Chem.* **2019**, *62*, 7751–7768.
[41] E. Vergara, S. Miranda, F. Mohr, E. Cerrada, E. R. T. Tiekink, P. Romero, A. Mendía, M. Laguna, *Eur. J. Inorg. Chem.* **2007**, *18*, 2926–2933.
[42] R. Gavara, J. Llorca, J. C. Lima, L. Rodríguez, *Chem. Commun.* **2013**, *49*, 72–74.
[43] E. Aguiló, R. Gavara, J. C. Lima, J. Llorca, L. Rodríguez, *J. Mater. Chem. C* **2013**, *1*, 5538.
[44] A. Pinto, G. Hernández, R. Gavara, E. Aguiló, A. J. Moro, G. Aullón, M. Malfois, J. C. Lima, L. Rodríguez, *New J. Chem.* **2019**, *43*, 8279–8289.
[45] M. Aydinli, M. Tutaş, B. Atasoy, Ö. A. Bozdemir, *React. Funct. Polym.* **2005**, *65*, 317–327.
[46] T. Shen, C. Guo, Y. Cao, Y. Lv, J. Zhang, C. Yuan, B. Zeng, G. Chen, Y. Xu, L. Dai, *ACS Appl. Polym. Mater.* **2021**, *3*, 5604–5611.
[47] E. Aguiló, L. Soler, A. Casanovas, A. J. Moro, J. C. Lima, L. Rodríguez, J. Llorca, *ChemCatChem* **2017**, *9*, 3289–3292.
[48] J. Andres, A. S. Chauvin, *Phys. Chem. Chem. Phys.* **2013**, *15*, 15981–15994.
[49] R. Gavara, A. Pinto, R. Donamaría, M. E. Olmos, J. M. López de Luzuriaga, L. Rodríguez, *Inorg. Chem.* **2017**, *56*, 11946–11955.
[50] J. M. López de Luzuriaga, M. Monge, M. E. Olmos, M. Rodríguez-Castillo, I. Soldevilla, D. Sundholm, R. R. Valiev, *Inorg. Chem.* **2020**, *59*, 14236–14244.
[51] A. Pinto, N. Svahn, J. C. Lima, L. Rodríguez, *Dalton Trans.* **2017**, *46*, 11125–11139.
[52] A. Gandioso, S. Contreras, I. Melnyk, J. Oliva, S. Nonell, D. Velasco, J. García-Amorós, V. Marchán, *J. Org. Chem.* **2017**, *82*, 5398–5408.
[53] I. Seven, T. Weinrich, M. Gränz, C. Grünewald, S. Brüß, I. Krstic¨, T. F. Prisner, A. Heckel, M. W. Göbel, *Eur. J. Org. Chem.* **2014**, *19*, 4037–4043.

Manuscript received: January 11, 2023
Revised manuscript received: February 11, 2023
Accepted manuscript online: February 17, 2023